

Article

Prediction of New Distillation-Membrane Separation Integrated Process with Potential in Industrial Application

Xin Ding, Xiaohong Wang *, Peng Du, Zenghu Tian and Jingxuan Chen

College of Chemical Engineering, Qingdao University of Science and Technology, Qingdao 266042, China; 2019010004@mails.qust.edu.cn (X.D.); 4020010009@mails.qust.edu.cn (P.D.); 4020010064@mails.qust.edu.cn (Z.T.); 4020010004@mails.qust.edu.cn (J.C.)

* Correspondence: xhwang@qust.edu.cn

Abstract: In this paper, a new integrated distillation-membrane separation process solution strategy based on genetic programming (GP) was established for azeotrope separation. Then, a price evaluation method based on the theory of unit membrane area was proposed, so that those membranes which are still in the experimental stage and have no actual industrial cost for reference can also be used in the experimental research. For different characteristics and separation requirements of various azeotropic systems, the solution strategy can be matched with difference pervaporation membranes, and the optimal distillation-membrane separation integrated process can be solved quickly and accurately. Taking methanol-toluene as an example, the separation operation was optimized by using the algorithm. The effects of different feed flows and compositions on the modification of the chitosan membrane were discussed. These results provide a reliable basis for the prospects for development and modification direction of membrane materials which are still in the experimental research stage.

Keywords: azeotrope separation; membrane modification; genetic programming; distillation-membrane separation integration



Citation: Ding, X.; Wang, X.; Du, P.; Tian, Z.; Chen, J. Prediction of New Distillation-Membrane Separation Integrated Process with Potential in Industrial Application. *Processes* **2021**, *9*, 318. <https://doi.org/10.3390/pr9020318>

Academic Editor: Iqbal M. Mujtaba
Received: 8 January 2021
Accepted: 5 February 2021
Published: 9 February 2021

Publisher's Note: MDPI stays neutral with regard to jurisdictional claims in published maps and institutional affiliations.



Copyright: © 2021 by the authors. Licensee MDPI, Basel, Switzerland. This article is an open access article distributed under the terms and conditions of the Creative Commons Attribution (CC BY) license (<https://creativecommons.org/licenses/by/4.0/>).

1. Introduction

The separation of the azeotropic system has always been a hot and difficult topic in the field of the chemical industry because the relative volatility is near to 1 at the azeotropic point [1,2]. As the most commonly used separation method in the chemical industry, the traditional distillation operation has its inherent limitations, which makes it difficult to directly separate the azeotrope system into high-purity products [3]. Similarly, other separation methods have their own disadvantages. Higher separation efficiency and lower separation cost are the goals of chemical companies and chemical researchers [4], and a single separation method is gradually difficult to meet the production needs. The integration process of different unit operations has become a research hotspot, and the integration process can maximize the advantages of them and avoid disadvantages.

In recent years, great progress has been made in the integration of membrane separation and traditional distillation [5,6]. Compared with the traditional distillation method, membrane separation has wider availability and higher flexibility [7,8]. For the separation of the system to be separated, using membranes made of different materials can get different optimal processes; and the results will be quite different when the same materials are modified in different directions [9]. This flexibility makes the integrated process of membrane separation and distillation have obvious advantages [10–12]. The integration of distillation and the membrane module is more economical. Khalid A [13] and others compared several schemes with different process structures, and the results showed that the combination of distillation and membrane separation could effectively reduce the production cost of bioethanol. Yu Congli [14] and others proposed an integrated process of distillation and the molecular sieve membrane for the production process of

ethanol dehydration, and compared it with the pressure swing distillation process. The results showed that the steam cost of the distillation membrane integrated process could be saved by 30%. Jin Hao [15] and others proposed an integrated process of the reactive distillation pervaporation membrane with side line for the acetic esterification process of ethyl acetate production, which could effectively improve the steam transfer efficiency. The results show that the energy of the new process can be saved by 26.6% compared with the traditional process. In addition, the integrated distillation membrane separation method is also commonly used to treat industrial wastewater. Wang Yun [16] and others found that the coupled process of reversible gas membrane and multi-effect membrane distillation can be applied to treat ammonia nitrogen in wastewater to obtain high purity concentrated ammonia water.

Although there have been many stage achievements in the research of the distillation membrane integration process, there are still two problems that are difficult to solve. One is that most experiments mainly focus on an azeotropic system, while the research on general separation methods for the azeotropic system is still blank. On the other hand, due to the different coupling degrees of distillation membrane integration, it is difficult to fully describe the complexity and diversity of the process structure. This complexity is also reflected in the difficulty of solving multi-objective optimization problems. Therefore, it is urgent to develop a general algorithm for the azeotropic system, and quickly search and solve the optimization of the distillation membrane separation process according to different separation requirements.

The genetic programming algorithm (GP) is an evolutionary algorithm [17], the main difference between GP and the genetic algorithm is that the former does not need to define the super structure in advance, and is more suitable for solving complex nonlinear programming problems caused by multiple uncertain factors, and the optimization problem of the integration process can also be solved well [18]. In the previous work, the research group has carried out some research on GP [19–21]. On this basis, the GP algorithm is proposed to solve the distillation and membrane separation problem [22]. The node definition, population generation, and genetic algorithm are optimized for the azeotrope system and membrane material, and the distillation membrane integrated solution strategy is established.

As the requirements for environmental protection, energy saving, and new membrane separation materials and performance in industrial production continue to increase, it is urgent to conduct a deeper study of these problems. In the integration of distillation and membrane separation, it is very important to choose the type and material of membrane. Generally, the types are divided into hydrophilic membrane and organic membrane, and membrane materials include: organic polymer membrane, inorganic molecular sieve membrane, various composite membranes, and so on. In order to make a profound study of the optimal membrane type, the membrane material and membrane characteristics in the integrated distillation membrane separation, an improved GP algorithm is proposed in this paper. The improved GP optimization algorithm is written in C++ language. Taking the methanol toluene system as an example, the chitosan membrane was integrated with the distillation column, and optimized by the improved GP algorithm. The influence of membrane modification on integrated optimization was discussed. The direction of membrane modification and future industrialization prospect were accurately predicted, which provided a solid foundation for the development of membrane science.

2. Improved GP Algorithm for Distillation-Membrane Separation Integration Process

In the early stage of the study, most of the pervaporation membranes selected by membrane separation nodes came from relatively mature commercial membranes with large-scale industrial applications, the main cause is that mature commercial membranes have more mature methods to estimate the cost. However, with the deepening of research, the main research goal of this paper is to study a large number of high-quality membrane materials which have not entered large-scale commercial applications and are still in

the experimental stage. Due to the diversity and variability of these membranes in the modification process, the GP algorithm has corresponding improvements in this paper. In order to accurately describe the influence of membrane performance on the optimal process and explore the direction of membrane modification, it is necessary to estimate the cost of the membrane. Therefore, an estimation system of membrane cost is proposed in this paper. The improved GP synthesis strategy used in this paper mainly focuses on expanding the characteristic parameters of membrane separation nodes, so as to describe the characteristics of the membrane more accurately and flexibly.

2.1. The Node Definition of Extended Distillation Column (D)

Firstly, in the new GP solution strategy, the definition of the distillation column node needs to be extended to better describe the optimal process searched and solved by the algorithm. The definitions are as follows.

- (1) The first characteristic parameter is (n_D), which represents the different discharge lines of the distillation column. The distillation column model used in the experiment is mainly one inlet and two outlets, so the feed stream is not defined separately. Each distillation column node has two outputs, one represents the top stream, the other is the bottom stream. If $n_D = 0$, it means the top stream; if $n_D = 1$, it means the bottom stream.
- (2) The second characteristic parameter is the number of theoretical plates (N). This value is generated randomly in a given range and used to solve the integrated process of the distillation membrane.
- (3) The third characteristic parameter is the ratio of reflux ratio to minimum reflux ratio (R_t). Similar to N , R_t is generated randomly in a given range.
- (4) The fourth characteristic parameter is the recovery rate of light components at the top of the column (η_D). This parameter is also generated randomly in a reasonable range.

Figure 1 is a schematic diagram of the extended distillation node and the corresponding distillation process.

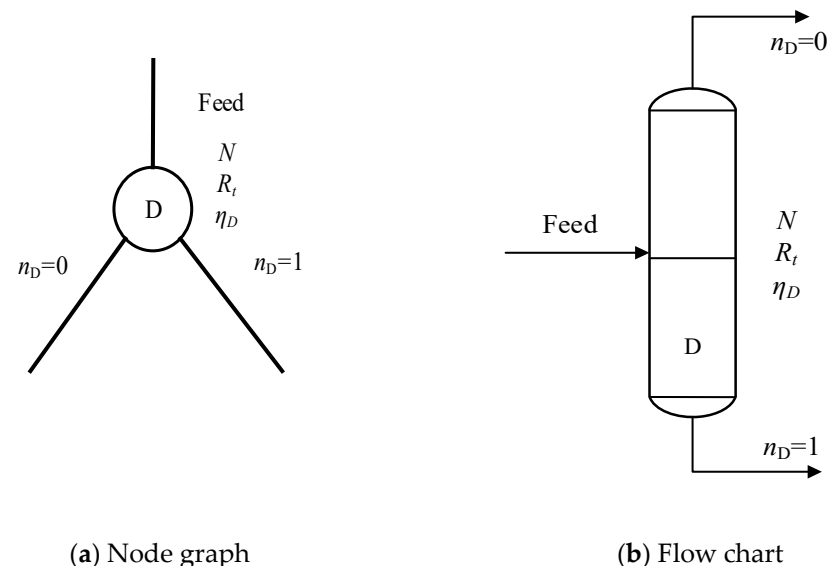


Figure 1. Distillation column node graph (a) and distillation module flow chart (b) obtained by decoding.

2.2. Extended Membrane Separation Node (M)

The main content of this section is the extended definition of the membrane separation node, including the performance parameters and separation parameters of the membrane, so as to better describe the properties of the membrane. The specific definition is as follows.

- (1) Structure parameter (n_M) is performance parameter. The membrane module is defined as a model of one inlet and two outlets. When $n_M = 0$, it represents the output flow of the residual side; when $n_M = 1$, it represents the output flow of the permeate side.
- (2) Experimental parameter (E_M) is also a performance parameter. Because the membrane selected in this paper is still in the experimental stage, it is necessary to add the operating temperature and thickness of the membrane to characterize the experimental conditions of the membrane.
- (3) The separation factor α and the following three parameters are all separation parameters. It refers to the ratio of the relative composition of the component in the outlet stream of the membrane to that in the feed stream, as defined in Formula (1) [9]. Y_B and Y_C represent the mass fractions of the two components on the permeate side respectively, and $Y_{B,F}$ and $Y_{C,F}$ represent the mass fractions of the two components in feed respectively:

$$\alpha = \frac{Y_B/Y_C}{X_{B,F}/X_{C,F}}. \quad (1)$$

- (4) Flux per unit membrane area J , the unit is $\text{kg}/(\text{m}^2 \cdot \text{h})$, as shown in Formula (2) [9], is the total mass of material per unit membrane area per unit time. m is the total mass of material passing through the membrane module in unit time (kg/h); a is the total membrane area of the current membrane module (m^2):

$$J = \frac{m}{A}. \quad (2)$$

- (5) The total area of the membrane is A_M , and the unit is m^2 . With the increase of A_M , the total flux of the membrane can be increased, and the processing capacity of the membrane module can be improved.
- (6) Further, the last one is membrane operating temperature (T), the unit is $^\circ\text{C}$. Its change may cause the performance of membrane materials and affect the separation performance of the membrane changed.

Figure 2 shows the node properties of membrane separation and the corresponding membrane separation operation diagram.



Figure 2. Membrane node graph (a) and membrane module flow chart (b) obtained by decoding.

The tree code generation rules, initial population generation, and termination criteria in the GP comprehensive solution strategy are all referred to in the previous work [22].

2.3. Membrane Cost Theory Prediction Method

In the preliminary study of the GP comprehensive strategy proposed in this paper, the pervaporation membrane with mature commercial applications is adopted as the main research object of the comprehensive solution strategy. Based on the above, this paper will further explore the membrane types and materials which are still in the experimental

research stage. Because there are many uncertainties in the cost estimation of this material in the future industry, there is no complete scientific method to predict at present, so it is difficult to calculate the fitness (defined as the annual total cost, TAC) of GP algorithm.

In view of the above situation, this paper proposed the upper limit price evaluation method by the unit membrane area (P_{max} , unit: $\$/(\text{m}^2 \cdot \text{year})$). Before the integrated optimization of distillation and membrane separation, the optimal value of TAC required by the traditional special distillation separation method for the separation system should be calculated. Then, in the integrated calculation of distillation and membrane separation, the price of unit membrane area can be predicted by adjusting the integrated system and using the membrane theory. The TAC value in distillation and membrane separation process is approximately equal to that in distillation separation. The price of the membrane obtained by unit membrane area theory predicts the P_{max} value of this kind of membrane. This parameter can be used to judge whether the membrane has industrial application value. The higher the P_{max} value is, the higher the feasibility of the membrane in the future industrial application is. The P_{max} value includes not only the manufacturing cost of the membrane, but also the annual operating cost of the membrane and the corresponding cost unit of membrane separation auxiliary equipment. The specific calculation steps of P_{max} are shown in Figure 3. Further, the specific calculation steps are as follows:

- (1) The special distillation method was used to establish a process to separate the separated system, and the process was optimized to obtain the optimal process and the corresponding TAC.
- (2) Set the initial value of the theoretical prediction price of the unit membrane area, and automatically calculate the fitness of individuals in the group.
- (3) The TAC of the optimal integrated process is compared with that of the special distillation process. If the difference between the two is less than the maximum allowable range, stop the calculation, then the theoretical predicted price of the unit membrane area is P_{max} ; if not, return to step (2), reset the theoretical predicted price of the unit membrane area and calculate individual fitness until P_{max} is obtained. The direction of price adjustment is determined by the difference of TAC between the two. If the difference is positive, the price per unit membrane area theoretically predicted will be reduced; otherwise, the price per unit membrane area theoretically predicted will be increased.

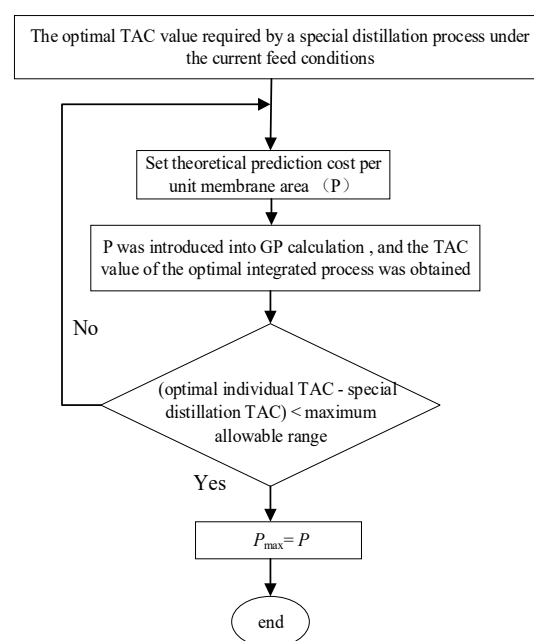


Figure 3. Flow chart of new genetic programming comprehensive solution strategy.

3. GP Algorithm Objective Function and Cost Model

The optimization objective function of the GP algorithm is defined as the total annual cost (TAC), including the equipment cost and operating cost of the distillation column and membrane module.

3.1. Cost Model of Distillation Column

The cost of the distillation column includes the cost of equipment and operation. The equipment cost mainly includes the cost of the column, the cost of the tray equipment, the cost of the condensers and the reboilers. The operating costs mainly include the consumption of cooling water of the condensers and that of the heating steam of the reboilers [23,24].

3.1.1. The Cost of Column (\$/year)

The estimation formula of column cost is shown in Formula (3) and (4):

$$\text{column cost} = \left(\frac{\text{M\&S}}{280} \right) \times 937.636 \times D_C^{1.006} \times H^{0.802} \times (2.18 + F_c), \quad (3)$$

$$H = \left(\frac{N}{0.75} - 3 \right) \times 0.6 + 6 \quad (4)$$

Among them, the M&S index is used to estimate the cost of chemical equipment, and the value is set as 1431.7 according to the data published in 2013; D_C is the diameter of the column, the unit is m; H is the height of the column, and the calculation formula is (4), the unit is m; $F_C = F_M \times F_P$, the column is made of stainless steel, so F_M is 3.67, and F_P is 1 in atmospheric column.

The tray cost is also estimated by M&S index, and the calculation formula is Equation (5):

$$\text{tray cost} = \left(\frac{\text{M\&S}}{280} \right) \times 97.243 \times D_C^{1.55} \times H \times (1 + 1.7). \quad (5)$$

The calculation of the cost of heat exchanger equipment is shown in (6)–(9):

A_H is the heat exchange area, the unit is m^2 , and the calculation formula is (6):

$$A_H = \frac{Q}{K \times \Delta t_m} \quad (6)$$

$$Q = \frac{W_h \Delta H_c}{3600 \times 1000} = \frac{W_c \Delta H_c}{3600 \times 1000} \quad (7)$$

$$\Delta t_m = \frac{\Delta t_1 - \Delta t_2}{\ln\left(\frac{\Delta t_1}{\Delta t_2}\right)} = \frac{(T_1 - t_1) - (T_2 - t_2)}{\ln\left(\frac{T_1 - t_1}{T_2 - t_2}\right)} \quad (8)$$

$$\text{Cost of heat exchanger equipment} = \frac{1}{3} \times \left(\frac{\text{M\&S}}{280} \right) \times 474.668 \times A_H^{0.65} (2.29 + 3.75 \times (1.35 + 0.8)) \quad (9)$$

A_H is the heat exchange area, the unit is m^2 ; Q is the heat load of the heat exchangers, the unit is kW; ΔH is the enthalpy difference of fluid heat exchange, the unit is kJ/kg; subscript c is cold fluid; K is the heat transfer coefficient; Δt_m is the heat transfer temperature difference, in this paper, the average logarithmic temperature difference is selected, the unit is $^{\circ}\text{C}$.

3.1.2. The Cost of Operation (\$/year)

The operation cost is composed of heating steam cost and cooling water cost, both of which come from utilities. There are three types of steam costs:

- (1) Low pressure steam (6 bar, 433 K) = 7.72 \$/GJ,
- (2) Medium pressure steam (11 bar, 457 K) = 8.22 \$/GJ,
- (3) High pressure steam (42 bar, 527 K) = 9.88 \$/GJ.

The calculation formula of cooling water cost in public works is shown in Formula (10):

$$\text{cooling water cost} = C_w \left(\frac{Q}{\Delta T_w \times C_p \times 1000} \right) \times 8000 \times 3600. \quad (10)$$

where C_w is the price of cooling water (3 \$/gcal); ΔT_w is the cooling water; the temperature difference between inlet and outlet is designed as 10 °C; C_p is the specific heat of water (4.183 kJ/(kg·K)).

3.2. Cost Model of Membrane Module Separation

The membrane module includes equipment cost and operating cost, the equipment cost is the cost of membrane material, production cost, and auxiliary equipment cost. The equipment cost of the commercial membrane is given by the manufacturer of the membrane. The operating cost mainly includes the energy consumption and maintenance cost of auxiliary equipment, and the maintenance cost is also given by the manufacturer.

Since the chitosan and polyurethane membranes studied in this paper have not been used in industry at present, the method proposed in Section 2.2 is used to estimate the theoretical upper limit price (P_{max} value) of all membrane costs.

4. Calculation of Industrial Examples

In this paper, a new GP comprehensive solution strategy for the distillation-membrane integration process was studied for the separation of the methanol-toluene azeotropic system, which was matched with the environmentally friendly chitosan membrane.

4.1. Optimization Calculation of Extraction Distillation Separation Process for Methanol-Toluene System

According to the individual fitness calculation rules of the new GP algorithm, the system was separated by special distillation, and the TAC value of the optimal process was calculated. In this paper, the extractive distillation was adopted, and O-xylene was selected as the extractant [25]. The purity of the products should be more than 99.5 wt%. The sequential iterative method [24] was adopted to optimize the extractive distillation process. Table 1 shows the corresponding optimal TAC values under different feed conditions. Figure 4 is one of the processes.

Table 1. Optimized calculation results of extractive distillation for the methanol-toluene azeotrope system.

Feed Flow/(kg/h)	Feed Composition/(methanol/wt %)	TAC/(k \$/year)
100	10	54.23
300	10	116.22
500	10	166.56
100	30	88.5
100	50	108.3

4.2. Optimization Calculation and Analysis of the Distillation-Membrane Separation Integration Process for Chitosan Membrane

Chitosan membrane is a kind of methanol permeable membrane, Tetraethoxysilane (TEOS) can be added as a crosslinking agent to reduce the flux slightly and improve the separation factor greatly [26]. In this paper, the value of separation factor α and flux J in two states due to modification of the chitosan membrane were calculated by regression analysis of experimental data provided in the literature, the calculation formulas are shown in (11)–(14). In these formulas, x_f represents the methanol concentration at the feed point of the membrane module (kg/kg).

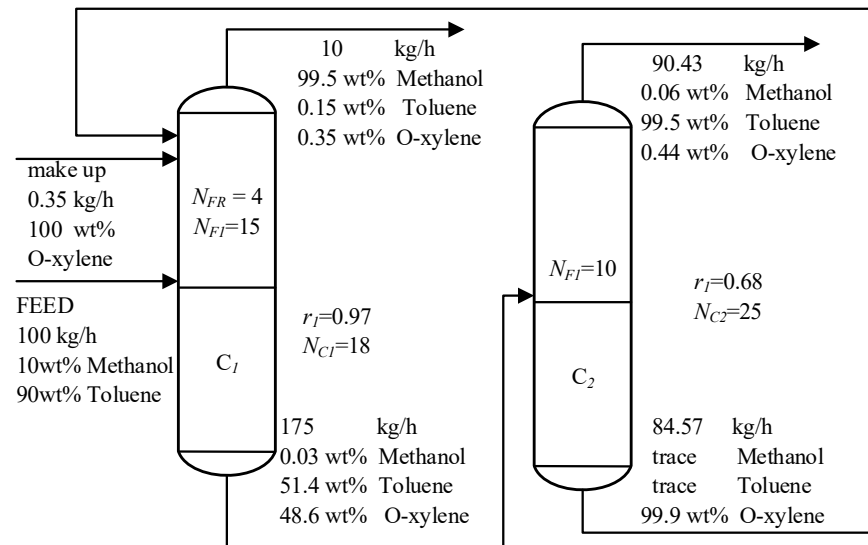


Figure 4. The optimal process and operation parameters when the feed flow rate is 100 kg/h and the methanol content is 10 wt%.

The formula of the modified pre-chitosan membrane:

$$\alpha = \begin{cases} 229.64e^{-5.481x_f} & x_f \leq 0.5 \\ 143.78e^{-3.883x_f} & x_f > 0.5 \end{cases}, \quad (11)$$

$$J = 0.1227x_f^2 + 0.0043x_f + 0.0975. \quad (12)$$

The formula of the modified chitosan membrane:

$$\alpha = \begin{cases} -6596.6x_f^3 + 9405.5x_f^2 - 4431.3x_f + 756.66 & x_f \leq 0.6 \\ 320.49e^{-2.608x_f} & x_f > 0.6 \end{cases} \quad (13)$$

$$J = 0.0523x_f^2 + 0.00437x_f + 0.0766. \quad (14)$$

4.3. Influence of Feed Flow on Chitosan Membrane Modification

In this section, the feed composition was fixed as methanol content of 10 wt%, and the feed flow rates of 100, 300, and 500 kg/h were studied. Using the chitosan membrane as the research object, it was found that no matter whether the membrane was modified or not, the optimal integrated process searched by the GP algorithm under three feed rates was the C-PV acyclic integrated process (the separation sequence is distillation-membrane), Table 2 shows the optimal integration of process parameters of the three kinds of feed flow rates in the case of unmodified membrane and modified membrane, and Figure 5 shows one of these cases.

Table 2. The optimal integrated process parameters are obtained by using the modified membrane and the modified membrane under three feed flow rates, when the methanol content of the feed is 10 wt%.

Membrane Type	Feed Flow (kg/h)	P_{max} (\$/m ² year)	N	r	A_{py} (m ²)	M_{cost} (k \$/year)	S_{cost} (k \$/year)	PV_{cost} (k \$/year)	T_{cost} (k \$/year)	TAC (k \$/year)
Chitosan membrane	100	131	6	1.3	259	2.5	17.5	33.9	20.0	53.9
	300	100	4	1.1	934	2.4	15.2	99.1	17.5	116.6
	500	84	4	0.7	1781	2.1	15.0	149.6	17.1	166.7
Modified chitosan membrane	100	246	4	0.6	152	2.0	15.0	37.3	16.9	54.2
	300	218	5	1.3	446	2.5	16.4	97.4	18.9	116.3
	500	198	6	1.3	741	2.5	17.5	146.7	20.0	166.7

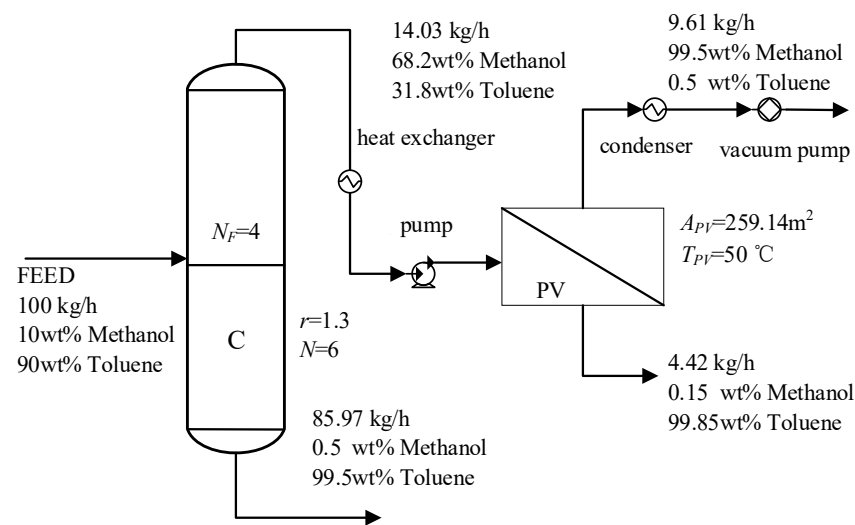


Figure 5. The optimal process structure and parameters of the chitosan membrane, when the feed flow rate is 100 kg/h and the methanol content is 10 wt%.

M_{cost} is the total operating cost except membrane module and its auxiliary equipment (the unit is k\$/year, the followings are the same), S_{cost} is the total equipment cost calculated by three-year depreciation period except membrane module and its auxiliary equipment. PV_{cost} is the total cost of membrane module and its auxiliary equipment per unit, and T_{cost} in the table is the total cost of distillation column and its auxiliary equipment.

The influence of feed flow on the optimal distillation-membrane separation integrated process is mainly reflected in the scale effect. The scale effect of distillation column leads to the increase of feed flow and the increase of the cost, which is also the reason why it plays an important role in large-scale industrial production. On the contrary, membrane separation has the advantage of low-flow because of the linear correlation between the treatment capacity and membrane area. Extractive distillation is similar to membrane separation, and the treatment capacity is related to the amount of extractant. This phenomenon leads to the difference of TAC change between extractive distillation column and conventional distillation column in integrated process. With the increase of feed flow, the cost of membrane separation module increases proportionally, while the cost of distillation column increases slightly. In order to make the TAC of integrated process similar to that of special distillation, the membrane separation module has to undertake more separation tasks, while the distillation column will undertake less separation tasks, this trend is also the solution direction of the comprehensive solution strategy.

According to the data in Table 2, the P_{max} values of modified membrane are higher under any feed flows. With the increase of feed flow, the P_{max} values of the two membranes decrease gradually. It can be found that the proportion of distillation column cost in TAC decreases gradually, which has been explained above. It is worth noting that the higher the feed flow, the less the cost of the distillation column in the optimal integration process by using the unmodified membrane, which is different from the results of the modified membrane. Comparing the two membranes, it can be found that the increase of membrane area of chitosan membrane is larger than that of modified chitosan membrane under any feed flow. In this case, it is not difficult to explain why the former has the phenomenon that the cost of distillation column is lower than that of low flow. At the same time, with the increase of feed flow, the decrease of P_{max} values of the modified chitosan membrane was lower than that of the unmodified chitosan membrane, indicating that the modified chitosan membrane can obtain higher income in dealing with higher feed flow.

4.4. Influence of Feed Composition on Chitosan Membrane Modification

In this section, the feed flow rate was fixed at 100 kg/h, and the research objects were methanol content of 10, 30, and 50 wt%. Compared with Section 4.3, the optimal process

is different under different feed compositions, when the feed content of toluene is 30 and 50 wt%, the searched optimal integration processes by using the GP algorithm are all the C-PV-PV structure (the two discharge streams of the distillation column are connected with the membrane module), Figure 6 shows one example.

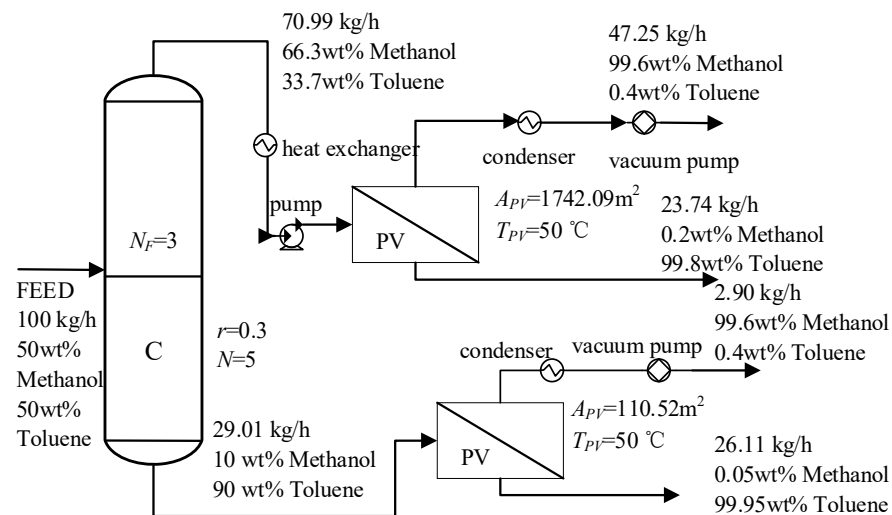


Figure 6. The optimal process structure and parameters of the chitosan membrane, when the feed flow rate is 100 kg/h and the methanol content is 50 wt%.

Table 3 shows the searched optimal integration process parameters under three feed compositions with two kinds of membrane modules. As we can see from the table, with the increase of methanol content in the feed, the P_{max} values of both membranes show a downward trend. The P_{max} values of the modified chitosan membrane under all the feed compositions are higher than that before modification, which indicates that the modified membrane could obtain higher profit under any feed compositions. However, when toluene content of feed is 50 wt%, the P_{max} value of modified membrane reduced greatly. As a result, not only the cost of the distillation column exceeded that before modification, but also the increase of the membrane area increased significantly, which indicated that the modified chitosan membrane did not have much advantage in treating feed composition higher than 50 wt%, and the improvement of the whole process benefit is mainly reflected in other ranges of feed compositions.

Table 3. The optimal integration process parameters of the three feed components are obtained by using the modified membrane, when the feed flow rate is 100 kg/h.

Membrane Type	Feed (Methanol Composition wt%)	P_{max} (\$/m ² year)	N	r	A_{PV} (m ²)	M_{cost} (k \$/year)	S_{cost} (k \$/year)	PV_{cost} (k \$/year)	T_{cost} (k \$/year)	TAC (k \$/year)
Chitosan membrane	10	131	6	1.3	259	2.5	17.5	33.9	20.0	53.9
	30	70	4	0.6	967	4.4	16.2	67.8	20.6	88.4
	50	46	5	0.3	1853	5.3	17.7	85.2	23.0	108.2
Modified chitosan membrane	10	246	4	0.6	152	2.0	15.0	37.3	16.9	54.2
	30	145	5	0.2	469	3.5	16.9	68.1	20.4	88.5
	50	54	11	9	1404	7.1	25.0	75.8	32.1	107.9

4.5. Summary

The P_{max} and the corresponding optimal distillation membrane separation integrated process parameters of the chitosan membrane before and after modification were calculated

under different flow rates and feed compositions. When the feed flow rate was 100 kg/h and the methanol content was 10 wt%, the optimal distillation membrane separation integrated process searched by the GP comprehensive solution strategy was the D-PV structure, and the P_{max} of the chitosan membrane before and after modification were 131 and 246 $\$/(\text{m}^2 \cdot \text{year})$, respectively. The D-PV-PV structure was found when the feed flow rate was 100 kg/h and the methanol content increased to 30 wt%. Through further analysis, it is concluded that the P_{max} enhancement effect of the modified chitosan membrane is not affected by the feed flow rate; the modified chitosan membrane has no obvious advantage in the range of 0–20 wt% methanol content in the feed.

5. Conclusions

In this paper, a GP comprehensive strategy was established for the rapid solution of the distillation-membrane separation integration process, and an evaluation system (P_{max} evaluation method) was proposed to predict the price based on the prediction theory of unit membrane cost.

- (1) The methanol-toluene azeotropic system was taken as an example to conduct an integrated optimization calculation by matching the chitosan membrane, and the change of membrane separation task in the integrated process of distillation membrane separation was studied from two aspects of feed flow and composition.
- (2) The calculation results show that the P_{max} evaluation method proposed in this paper can provide a clear quantitative index for membranes (even the membranes that are in the experimental stage) to explore which modification direction of the membrane is more practical, that is, it can predict the economic benefits of membrane modification in its future industrialization, and thus provide a strong basis for the development of membrane material modification.

Author Contributions: Conceptualization, X.W.; Data curation, X.D.; Funding acquisition, X.W.; Methodology, X.W.; Software, P.D., Z.T. and J.C.; Writing—original draft, X.D.; Writing—review & editing, X.D. All authors have read and agreed to the published version of the manuscript.

Funding: This research was funded by National Natural Science Foundation of China, grant number 21676151.

Institutional Review Board Statement: Not applicable.

Informed Consent Statement: Not applicable.

Data Availability Statement: Data is contained within the article.

Conflicts of Interest: The authors declare no conflict of interest.

References

1. Widagdo, S.; Seider, W.D. Journal review. Azeotropic distillation. *AIChE J.* **1996**, *42*, 96–130. [[CrossRef](#)]
2. Qi, J.; Li, Y.F.; Xue, J.X.; Qiao, R.Q.; Zhang, Z.S.; Li, Q.S. Comparison of heterogeneous azeotropic distillation and energy-saving extractive distillation for separating the acetonitrile-water mixtures. *Sep. Purif. Technol.* **2020**, *238*, 116487. [[CrossRef](#)]
3. Muhammad, A.Z.; Muhammad, F.I.Z.; Munawar, Z.S.; Kamarul, A.I.; Mohd, K.A.H. Economic, Feasibility, and Sustainability Analysis of Energy Efficient Distillation Based Separation Processes. *Chem. Eng. Trans.* **2019**, *72*, 109–114.
4. Ahadi, H.; Karimi-Sabet, J.; Shariaty-Niassar, M.; Matsuurac, T. Experimental and numerical evaluation of membrane distillation module for oxygen-18 separation. *Chem. Eng. Res. Des.* **2018**, *132*, 49–504. [[CrossRef](#)]
5. Takehiro, Y.; Miki, Y.; Nobuo, H.; Hideyuki, N. Heat-Integrated Hybrid Membrane Separation–Distillation Process for Energy-Efficient Isopropyl Alcohol Dehydration. *J. Chem. Eng. Jpn.* **2018**, *51*, 890–897.
6. Qasim, F.; Shin, J.S.; Cho, S.J.; Park, S.J. Optimizations and heat integrations on the separation of toluene and 1-butanol azeotropic mixture by pressure swing distillation. *Sep. Sci. Technol.* **2016**, *51*, 316–326. [[CrossRef](#)]
7. Wu, Z.Q.; Zhang, C.; Peng, L.; Wang, X.R.; Kong, Q.Q.; Gu, X.D. Enhanced Stability of MFI Zeolite Membranes for Separation of Ethanol/Water by Eliminating Surface Si-OH Groups. *ACS Appl. Mater. Interfaces* **2018**, *10*, 3175–3180. [[CrossRef](#)]
8. Mansoor, K. Multi-stage synthesis of nanopore NaA zeolite membranes for separation of water/Ethanol mixtures. *Int. J. Res. Eng. Innov.* **2017**, *6*, 42–46.
9. Yao, L.L.; Xi, T.; Ye, H.; Hao, W.T.; Cui, P. Influence of n-alkyl methacrylate on the structure and properties of waterborne polyurethane membrane. *Membr. Sci. Technol.* **2017**, *37*, 1–8.

10. Fontalvo, J.; Keurentjes, J.T.F. A hybrid distillation–pervaporation system in a single unit for breaking distillation boundaries in multicomponent mixtures. *Chem. Eng. Res. Des.* **2015**, *99*, 158–164. [[CrossRef](#)]
11. Wang, C.; Zhang, Z.S.; Zhang, X.K.; Gao, J.; Stewart, B. Energy-saving hybrid processes combining pressure-swing reactive distillation and pervaporation membrane for n-propyl acetate production. *Sep. Purif. Technol.* **2019**, *221*, 1–11. [[CrossRef](#)]
12. Xiong, B.W.; Wu, H.D.; Zhou, Z.H. Research progress of organic-inorganic hybrid membranes for pervaporation. *Fine Chem. Eng.* **2020**, 1–8. [[CrossRef](#)]
13. Khalid, A.; Aslam, M.; Qyyum, M.A.; Faisal, A. Membrane separation process for dehydration of bioethanol from fermentation broths: Recent developments, challenges, and prospects. *Renew. Sustain. Energy Rev.* **2019**, *105*, 427–443. [[CrossRef](#)]
14. Yu, C.L.; Guo, H.C.; Ji, Z.H. Economic feasibility analysis on application of zeolite membrane in bio-based fuel ethanol production. *Mod. Chem. Ind.* **2019**, *39*, 192–194.
15. Jin, H.; Lu, J.W.; Tang, J.H.; Zhang, Z.X.; Fei, Z.Y.; Liu, Q.; Chen, X.; Cui, M.F.; Qiao, X. Simulation and analysis of a side stream reactive distillation- pervaporation integrated process for ethyl acetate production. *Acta Chem. Sin.* **2018**, *69*, 3469–3478.
16. Wang, Y.; Qin, Y.J.; Hao, X.G.; Li, H.Q.; Cui, D.S.; Liu, L.Q.; Liu, J. Reversible gas membrane process-multiple effect membrane distillati distillation process for removing ammonia from aqueous solution an producing aqueous ammonia. *Acta Chem. Sin.* **2015**, *66*, 3588–3596.
17. Koza, J.R. Genetic Programming II: Automatic Discovery of Reusable Programs. *Artif. Life* **2014**, *1*, 439–441.
18. Wang, X.H.; Li, Y.G. Intergration of Multicomponent products separation sequences via stochastic GP method. *Ind. Eng. Chem. Res.* **2008**, *47*, 8815–8822. [[CrossRef](#)]
19. Wang, X.H.; Hu, Y.D.; Li, Y.G. Synthesis of nonsharp distillation sequences via genetic programming. *Korean J. Chem. Eng.* **2008**, *25*, 402–408. [[CrossRef](#)]
20. Wang, X.H.; Li, Y.G.; Hu, Y.D. Intergration of heat-integrated complex distillation systems via Genetic Programming. *Comput. Chem. Eng.* **2008**, *32*, 1908–1917. [[CrossRef](#)]
21. Wang, X.H.; Li, Y.G. Stochastic GP intergration of heat integrated nonsharp distillation sequences. *Chem. Eng. Res. Des.* **2010**, *88*, 45–54. [[CrossRef](#)]
22. Wang, X.H.; Li, M.G.; Zhang, Y.P.; Hong, J.; Li, W.K.; Ding, X.; Li, Y.G. Research on the integration process of energy saving distillation-membrane separation based on genetic programming to achieve clean production. *Chem. Eng. Process. Process Intensif.* **2020**, *151*, 107885. [[CrossRef](#)]
23. Luyben, W.L. *Distillation Design and Control Using Aspen Simulation*; John Wiley & Sons: Hoboken, NJ, USA, 2013.
24. Tian, P. Process Design and Control of Acetonitrile-n-Propanol Azeotropic System by Special Distillation. Master’s Thesis, Qingdao University of science and technology, Qingdao, China, 2016.
25. Zhang, L.; Zhang, J.W.; Zhu, H.J. Separation of methanol toluene azeotrope by extractive distillation. *Chem. Ind. Eng.* **2013**, *30*, 71–75.
26. Mouilk, S.; Bukke, V.; Satta, S.C. Chitosan-polytetrafluoroethylene composite membranes for separation of methanol and toluene by pervaporation. *Carbohydr. Polym. Sci. Technol. Asp. Ind. Important Polysacch.* **2018**, *69*, 28–38. [[CrossRef](#)] [[PubMed](#)]